

# Stochastic and genetic factors influence tissue-specific decline in ageing *C. elegans*

Laura A. Herndon\*, Peter J. Schmeissner\*, Justyna M. Dudaronek\*, Paula A. Brown\*, Kristin M. Listner\*, Yuko Sakano\*, Marie C. Paupard†, David H. Hall† & Monica Driscoll\*

\* Department of Molecular Biology and Biochemistry, Rutgers, The State University of New Jersey, A232 Nelson Biological Laboratories, 604 Allison Road, Piscataway, New Jersey 08854, USA

† Department of Neuroscience, Albert Einstein College of Medicine, 1410 Pelham Parkway, Bronx, New York 10461, USA

The nematode *Caenorhabditis elegans* is an important model for studying the genetics of ageing, with over 50 life-extension mutations known so far. However, little is known about the pathobiology of ageing in this species, limiting attempts to connect genotype with senescent phenotype. Using ultrastructural analysis and visualization of specific cell types with green fluorescent protein, we examined cell integrity in different tissues as the animal ages. We report remarkable preservation of the nervous system, even in advanced old age, in contrast to a gradual, progressive deterioration of muscle, resembling human sarcopenia. The *age-1(hx546)* mutation, which extends lifespan by 60–100%, delayed some, but not all, cellular biomarkers of ageing. Strikingly, we found strong evidence that stochastic as well as genetic factors are significant in *C. elegans* ageing, with extensive variability both among same-age animals and between cells of the same type within individuals.

In *C. elegans*, many single-gene mutations confer significant extensions of lifespan<sup>1</sup>. Life-prolonging mutations affect several aspects of nematode biology, including insulin-like signalling for dauer larvae development, the development and function of sensory neurons, the consumption of food, and biochemical defences against stresses such as heat shock and reactive oxygen species (reviewed in refs 2, 3). However, a detailed understanding of the molecular and cellular events influencing longevity remains a central mystery in the biology of ageing. Similarly, factors that regulate healthspan (the adult period of unimpaired activity and function that precedes age-related decline) have not been well defined, despite their potential as targets for forestalling the deleterious consequences of ageing.

A major gap in our understanding of *C. elegans* ageing is the question of what happens to cell and organ systems over time. The paucity of information regarding the cellular consequences of ageing is striking, given that each of the 959 somatic cells in the mature *C. elegans* hermaphrodite is an identified cell of known ancestry<sup>4</sup>, which can be readily visualized in the living animal by using reporters labelled with green fluorescent protein (GFP), and that the reconstruction of full-animal serial section electron micrographs has documented the subcellular architecture of most cells<sup>5</sup>. To facilitate the elaboration of ageing mechanisms and to extend our understanding of tissue-specific contributions to healthspan and longevity, we characterized major cellular changes that accompany *C. elegans* ageing by using fluorescence and electron microscopic techniques.

## A stochastic component to age-related locomotory decline

With abundant food at 20 °C, *C. elegans* develops from an embryo to sexual maturity in approximately 3 days, lays virtually all of its eggs over the first 3–4 days of adulthood, and then persists through a post-reproductive period during which senescent decline is evident (mean lifespan approximately 12–18 days)<sup>6</sup>. To lay the groundwork for a detailed analysis of cellular changes that comprise ageing in *C. elegans*, we first examined the appearance of wild-type animals over time using Nomarski differential-interference-contrast optical microscopy. In addition to an accumulation of dark pigment and

lipofuscin within the body<sup>6,7</sup>, vacuole-like structures, visually similar to neurons that die in response to ion channel injury<sup>8</sup>, first appear in nematode bodies towards the end of the reproductive period, and increase in size and number over time (Supplementary Fig. 1a). These vacuolar structures occur in variable positions and with a variable time of onset.

Our initial look at ageing populations also suggested significant heterogeneity in mobility of same-age individuals; we therefore

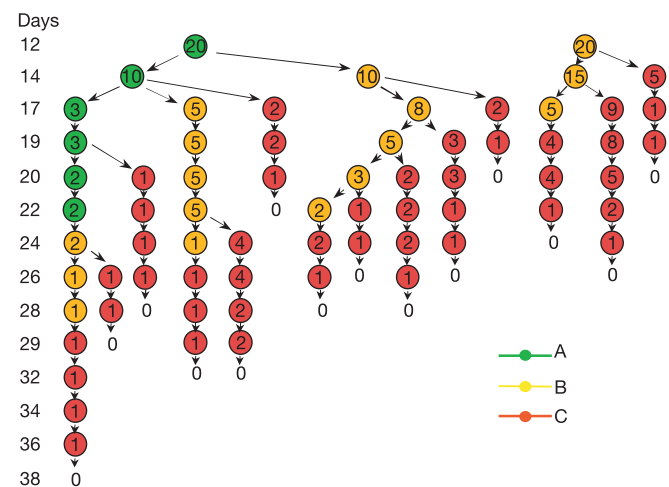


**Figure 1** Behavioural phenotypes of ageing nematodes indicate progressive decline with stochastic onset and variable rates. Twelve days after a synchronized egg lay, we categorized 40 wild-type animals on the basis of their locomotory phenotypes A (green), B (yellow) and C (red). We reclassified individuals every 1–3 days until all animals had died. Numbers within the circles represent animals scored in a given class on a particular day. Similar results were observed in four additional independent trials. Of 217 class A animals, 194 proceeded through stages B and then C before death. Similarly, 254 of 262 class B animals became class C animals before dying. We never observed a reversal of class order (B to A or C to B).

characterized locomotion in ageing populations in detail. We scored age-synchronized individuals both for spontaneous movement and for response to prodding with a wire at various points during adulthood. Somewhat unexpectedly for an isogenic population, we could distinguish three classes of behavioural phenotypes in a same-age population late in the lifespan. In one class, animals move constantly and leave sinusoidal tracks in the *Escherichia coli* lawn through which they migrate. These highly mobile animals, which we designate as class A, respond to prodding by vigorous movement away from the touch stimulus. Members of class B do not move unless prodded and leave tracks that are non-sinusoidal, reflecting uncoordinated locomotion. Class C animals do not move forward or backward even when prodded but do exhibit head and/or tail movements or twitch in response to touch. These classifications are broad enough for the vast majority of nematodes to be fitted into a single class after one observation. Although borderline cases did arise, class was typically clear by the next score point. All animals begin adulthood in class A. Class B animals first appear in the population at about day 6–7, which coincides approximately with the end of the reproductive period under laboratory conditions at 20 °C. Class C animals first appear at about day 9–10 (Supplementary Fig. 1b).

To gain a better understanding of the origin of the diversity of age-related behavioural classes, we followed hundreds of individuals over time. We sorted age-synchronized animals by class and re-scored for class every 1–3 days until death (Fig. 1 shows data from one representative trial). This analysis confirmed that age-associated locomotory defects increase progressively in severity over time<sup>7,9</sup>, and established that age-related behavioural changes occur with different times of onset and progress at different rates of decline in individual animals. We found that behavioural class is a

better predictor of life expectancy than chronological age (Supplementary Fig. 1c).

That both the individual time of onset and the rate of behavioural decline are widely variable among isogenic members of a same-age population reared under the same environmental conditions indicates that at least one major factor in the behavioural ageing of *C. elegans* is stochastic.

### Intactness of the nervous system in old nematodes

We initially sought evidence of age-related neurodegeneration in *C. elegans* because diminished locomotory responses could result from neuronal structural deterioration or cell death, and because the vacuolar structures in ageing nematodes superficially resemble necrotic-like neuronal cell deaths<sup>10</sup>. We used GFP reporters to visualize specific groups of neurons from comparably aged, or comparably categorized (locomotory classes A, B or C), nematodes over the lifespan.

Examination of animals expressing an integrated promoter for the *unc-119* gene that expresses GFP ( $p_{unc-119}$ GFP) array in all neurons<sup>11</sup> (3–4-day-olds ( $n = 14$ ), 6–9-day-olds ( $n = 29$ ) and 12–16-day-olds ( $n = 15$ )) revealed that all major structures of the *C. elegans* nervous system, including dorsal and ventral nerve cords, neuronal commissures that cross the body, lateral neurons and the nerve ring<sup>5</sup>, remain clearly distinguishable throughout the lifespan. Even in 15 late-stage class C animals ( $n = 7$  14-day-olds;  $n = 8$  18-day-olds), neuronal processes were positioned and extended similarly to those in young animals (data not shown). For a more detailed analysis of individual neurons, we scored animals harbouring an integrated  $p_{mec-4}$ GFP array expressed in six body touch-sensing neurons<sup>12</sup> and found that, without exception, we could easily distinguish normal cell bodies and processes at all

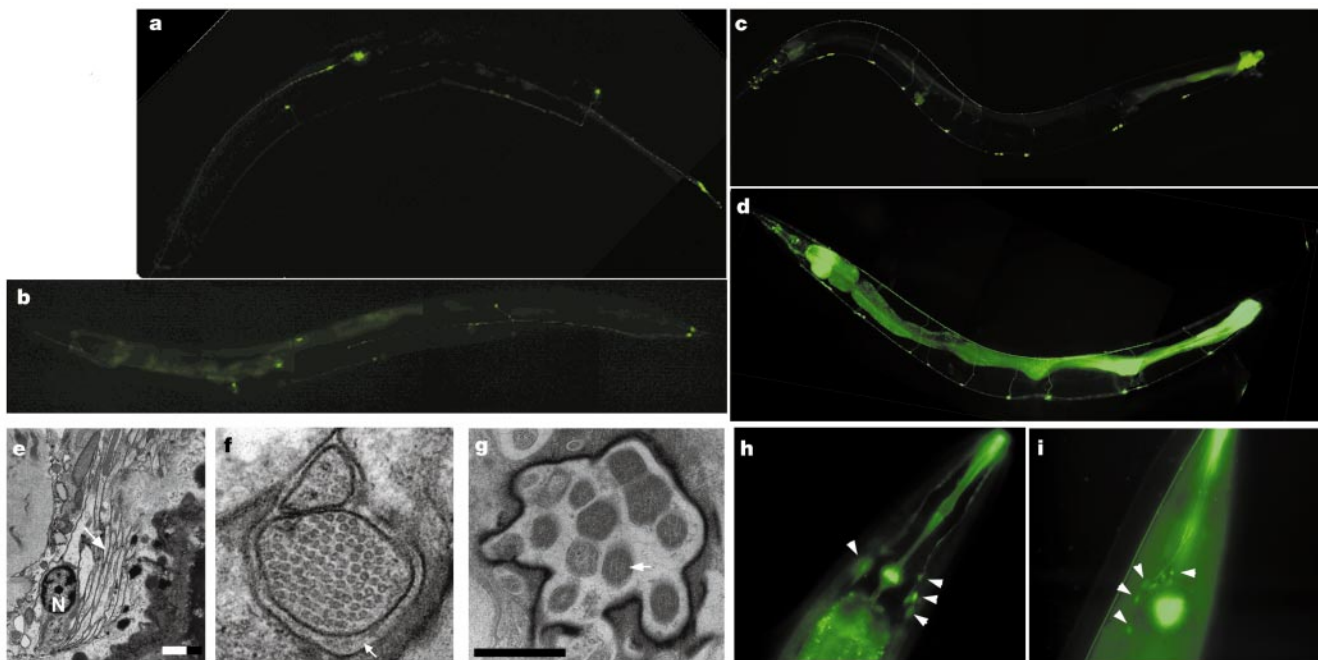


**Figure 2** The integrity of the nervous system is maintained in ageing nematodes. **a, b**, Six touch neurons were revealed with an integrated  $p_{mec-4}$ GFP reporter; examples of young (**a**, day 4) and old (**b**, day 15) adults are shown. **c, d**, Eleven DA and DB motor neurons were revealed with a  $p_{unc-129}$ GFP reporter; examples of young (**c**, day 4) and old (**d**, day 15) animals are shown. At every time point, the 11 neurons scored could be identified and processes appeared intact (day 4,  $n = 77$  worm/847 cell observations; day 15,  $n = 82$  worm/902 cell observations). Background intestinal autofluorescence is also apparent and increases with age. **e**, Section through a day 18 class C animal reveals processes in the nerve cord (white arrow) and a neuronal nucleus (N) that are

ultrastructurally similar to those in younger animals. Scale bar, 1  $\mu$ m. **f**, Touch neurons maintain characteristic features such as prominent 15-protofilament microtubules (circular in cross-section) and an extracellular mantle that borders the neuron process (white arrow), even in a day 18 class A animal. Scale bar, 0.1  $\mu$ m. **g**, Electron micrograph of an amphid cross-section reveals ciliated dendrites of all 12 amphid neurons (arrow indicates one of these) in a class B animal. Scale bar, 0.5  $\mu$ m. **h, i**, A subset of amphid sensory neurons are open to the environment, and neurons fill with dye in both young (**h**, day 4) and old (**i**, day 24, class C) animals. Arrowheads indicate filled cell bodies.

timepoints ( $n = 180$  animals; 1,080 total cell observations; Fig. 2a, b). In 20 decrepit C-stage animals, we found six touch neurons intact in every animal (120 total cell observations). We also used an integrated  $p_{unc-129}GFP^{13}$  reporter to examine the number and integrity of the DA and DB motor neurons (which innervate body wall muscle) and found all scored neurons detectable with commissures intact (2,453 total neurons evaluated;  $n = 77$  4–6-day-olds;  $n = 64$  8–10-day-olds;  $n = 82$  12–17-day-olds; Fig. 2c, d). Similarly, 14 class C animals of various chronological ages ( $n = 7$  15-day-olds;  $n = 5$  19-day-olds;  $n = 2$  30-day-olds) had DA and DB motor neurons indistinguishable from DA and DB neurons in

younger adults (data not shown). In sum, a detailed examination of representative sensory and motor neurons failed to indicate any signs of neuronal degeneration associated with either advanced *C. elegans* age or extensive behavioural decline.

We also examined thin-section electron micrographs derived from 18-day-old nematodes of behavioural classes A, B and C and compared them with the extensive collection of electron micrographs of young adult animals available at the Center for *C. elegans* Anatomy. This survey identified intact neurons even in class C animals and failed to produce any evidence of widespread degeneration in the nervous system. The nerve rings and longitudinal nerves

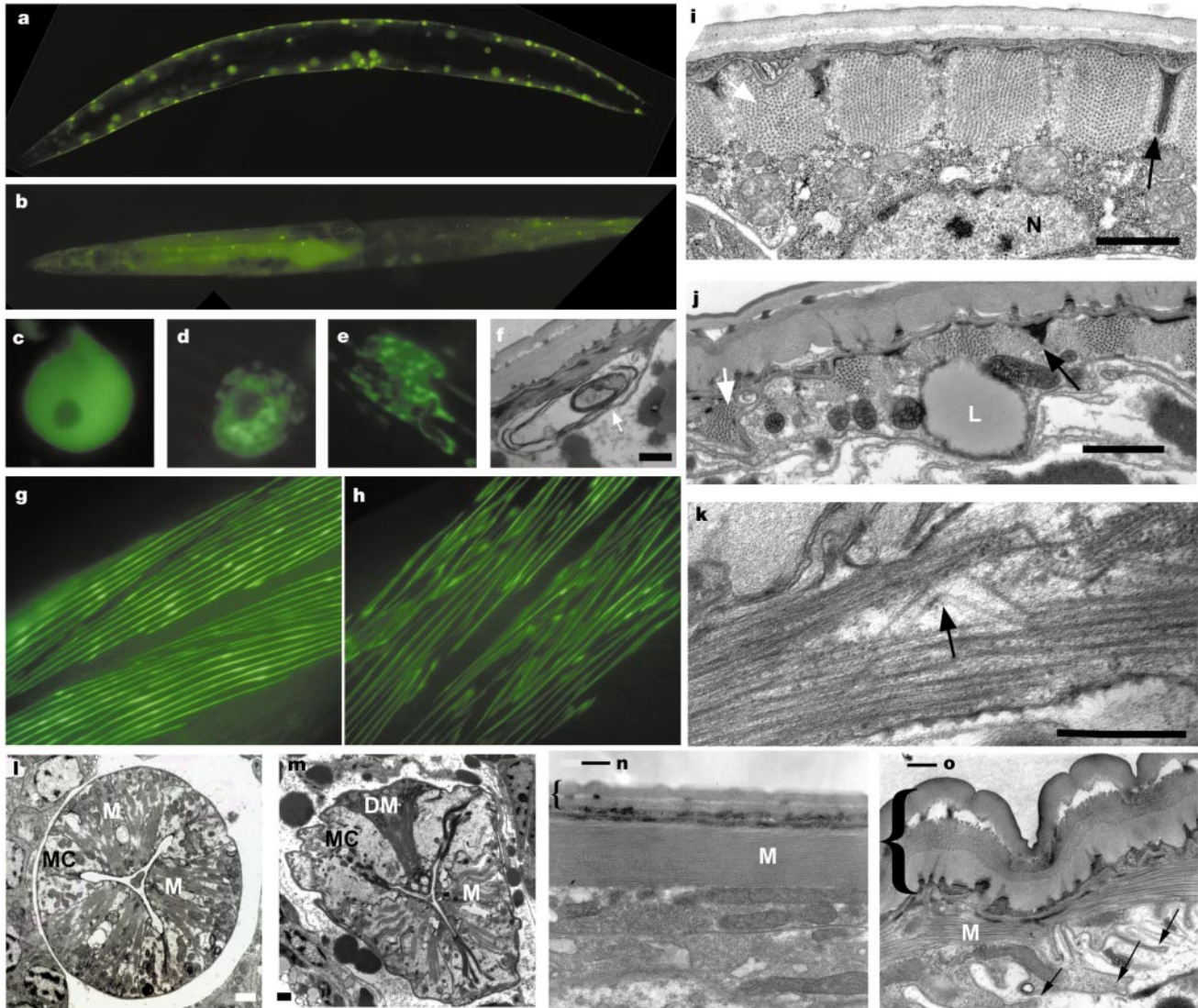


**Figure 3** Age-related deterioration of *C. elegans* body wall muscle. **a, b**, Whole-animal view of nematodes expressing GFP localized to the nuclei of body wall muscle (**a**, day 8; **b**, day 14; anterior to the left). The apparent disappearance of signal seen at  $\times 50$  magnification actually reflects the conversion of nuclear GFP to a fragmented pattern (see **e**). **c–e**, Magnified ( $\times 1,000$ ) view of muscle nuclei as revealed by GFP (**c**, day 7; **d**, day 12, appearance of small, dark patches and an increase of size of the nucleolus; **e**, day 18, fragmented phase). **f**, Example of a rare muscle nucleus (arrow) undergoing autophagy; day 18, class B. Scale bar,  $1 \mu\text{m}$ . **g, h**, Body wall muscle sarcomeres as detected by a  $p_{myo-3}MYO-3/GFP$  translational fusion, highlighting myosin heavy chain A (**g**, day 4; **h**, day 18, class B). **i–k**, Electron micrographs of body wall muscle, scales as indicated. **i**, Cross-section through a single muscle quadrant of a day 4 animal. Sarcomeres (white arrow) interface with the hypodermis and cuticle via dense bodies (black arrow). Scale bar,  $1 \mu\text{m}$ . **j**, Cross-section through single muscle of a day 18 class B animal with prominent

lipid inclusion (L). Note the loss of cytoplasmic volume and loss of myosin thick filaments (white arrow), but a retention of actin and dense bodies that interface with the hypodermis and cuticle (black arrow). Scale bar,  $1 \mu\text{m}$ . **k**, Magnified view of a frayed sarcomere in which myosin filaments are severely bent (arrow), from a day 18 class B animal. Scale bar,  $0.5 \mu\text{m}$ . **l**, Cross-section of a circular pharynx from a young adult (day 4) showing three-fold symmetry of muscle (M), marginal cells (MC) and open lumen. Scale bar,  $1 \mu\text{m}$ . **m**, Cross-section of the pharynx of a day 18 class B adult (MC, marginal cell; M, muscle; DM, deteriorated muscle). Scale bar (lower left),  $1 \mu\text{m}$ . **n, o**, Comparison of cuticle in young (day 4 class A, **n**) and day 18 class B (**o**) animals. Panels are at the same scale and thus the cuticle (marked by curly brackets) clearly shows differences in thickness. Disorganization of underlying muscle (M) and shedding of cytoplasm (cell fragmentation) through thin basal extensions from muscle (arrows) is also apparent in **o**. Scale bars,  $0.5 \mu\text{m}$ .

of the ventral and dorsal nerve cords were well formed (Fig. 2e), and touch receptor neurons were filled with characteristic 15-protofilament microtubules and surrounded by specialized extracellular matrix typical of younger neurons (Fig. 2f). We could readily identify all 12 amphid sensory neurons of the nose (some of which have been implicated in lifespan regulation<sup>14</sup> (Fig. 2g)), and the ciliated amphid neurons were morphologically normal. Even in 18 decrepit class C animals, the chemosensory amphid neurons that open to the environment fill with dyes comparably to their younger counterparts<sup>15</sup> (Fig. 2h, i). Microtubule bundles and neuronal nuclear structures were generally maintained. The only subtle changes we noted were a slight increase in cytoplasmic electron density and a modest reduction in neurite calibre in older animals (slightly narrower in class C than in class B; data not shown).

Overall, our study of the ageing *C. elegans* nervous system indicates, first, that there is little if any neuronal cell death during the *C. elegans* lifespan, even in severely compromised animals; and second, that there is no large-scale age-associated loss or restructuring of neurites or nuclei. Although we cannot rule out significant changes in biophysical properties (nerve conduction, synaptic

transmission), it is clear that at the cellular level the nervous system is well maintained in senescing *C. elegans*.

### Sarcopenia in ageing nematodes

Progressive locomotory impairment during *C. elegans* ageing could be the consequence of a decline in muscle function. We screened for evidence of age-related muscle deterioration by monitoring GFP-tagged proteins localized to either body wall muscle nuclei ( $p_{myo-3}$ GFP/NLS) or sarcomeres ( $p_{myo-3}$ MYO-3/GFP). We noted an apparent decrease, beginning in mid-life, in the number of GFP-labelled nuclei detectable under low-power magnification ( $\times 50$ ), with class C animals exhibiting the most extreme signal loss (Fig. 3a, b). A higher-resolution examination ( $\times 1,000$ ) indicated that this 'loss' reflects a striking change in the distribution of the nuclear-localized GFP fluorescence over time (Fig. 3c–e). Starting at day 7, small, dark patches begin to appear within many muscle nuclei (Fig. 3c). Also at day 7, the nucleus and nucleolus begin to lose circularity and become more misshapen. Another trend indicated by our nuclear GFP survey and supported by electron-microscopic data is that nucleolar size seems to increase relative to nuclear size with age (in day 7 animals, the ratios of nucleolar size to nuclear size as quantified by NIH Image were  $0.16 \pm 0.01$  (mean  $\pm$  s.e.m.) but at day 18 they were  $0.30 \pm 0.02$  (mean  $\pm$  s.e.m.)) (Fig. 3c–e; Supplementary Fig. 2a). The degree of GFP mottling increases progressively over the lifespan (Fig. 3d), so that later in life GFP fluorescence can acquire a highly fragmented appearance (Fig. 3e). The degree of nuclear change seems to correlate with locomotory class (Supplementary Fig. 2b) and to reflect changes in nuclear GFP distribution rather than nuclear breakdown, because ultrastructural electron-microscopic examination revealed nuclear breakdown only rarely (less than 2% of all muscle cells examined; Fig. 3f). Significantly, at most mid-life and late-life time points (days 9–20), we found that nuclear GFP distribution in different muscle cells within individual animals was variable (for example, ranging from non-mottled to severely mottled), indicating that stochastic factors might influence age-related nuclear changes in muscle on a cell-by-cell basis (Supplementary Fig. 2a).

Our analysis of a GFP-tagged MYO-3 protein<sup>16</sup> that is localized to the sarcomeres of body wall muscle revealed that, whereas in young animals sarcomeres are organized in tight parallel symmetric rows (Fig. 3g), sarcomeres in older animals seem progressively disorganized with less dense packing and irregular orientation (Fig. 3h). In some individual muscles we noted marked changes in sarcomere orientation or a fraying of individual sarcomeres into thinner, misdirected strands. However, the MYO-3/GFP protein labels sarcomeres until the end of the lifespan, and thus muscles do not fully disintegrate during *C. elegans* ageing.

Age-related decline in sarcomere integrity was more marked as viewed by electron microscopy. Sarcomeres clearly become more disorganized in old muscle (Fig. 3i, j) and include significantly fewer myosin thick filaments per sarcomere unit. Within some muscles of day 18 animals, individual thick filaments appear to bend abnormally and break (Fig. 3k). We also found a striking and prevalent shrinkage of the muscle cells, due in large part to a progressive cytoplasmic loss. The plasma membrane becomes highly invaginated and fragments can be shed from the muscle belly (Fig. 3i, j; also apparent in Fig. 3n, o). We noted cytoplasmic loss even in class A animals, with loss more pronounced in classes B and C. Large lipid droplets accumulate within the muscle of aged animals (Fig. 3j). By contrast, dense bodies in muscle (attachment sites analogous to vertebrate focal adhesion sites that serve as the physical link between myofibrils and muscle membrane, the hypodermis and cuticle) are generally well maintained (Fig. 3i, j; Supplementary Fig. 3).

Muscle deterioration in ageing animals is not limited to body wall muscle. With increasing age the pharynx loses its smooth, rounded shape and takes on an irregular appearance. Myofibrils in individual pharyngeal muscles are lost over time. In addition, entire pharynx-

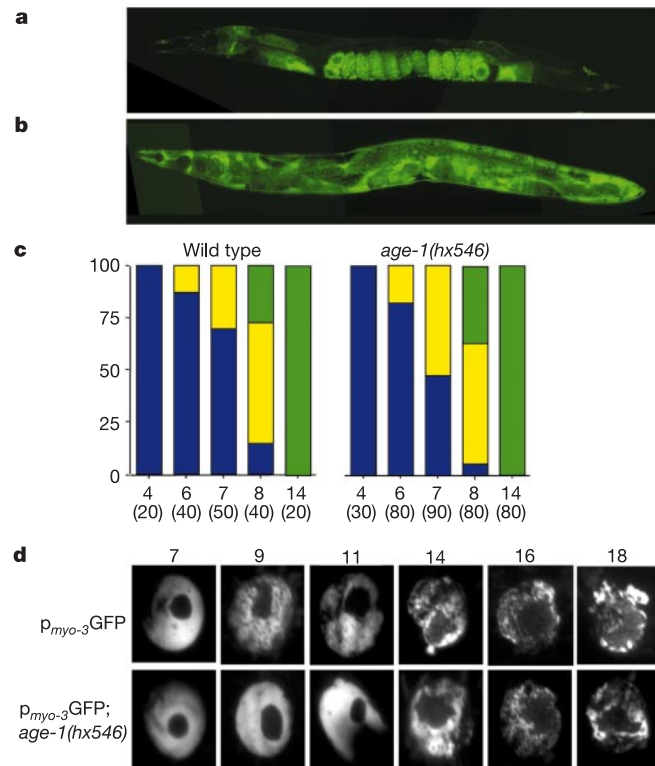


**Figure 4** The long-lived *age-1* mutant is not altered in age-related yolk protein redistribution but does exhibit delayed sarcopenia. **a, b**, Animals expressing tagged yolk protein, YP170/GFP: **a**, day 4 adult with yolk localized to developing embryos and intestine; **b**, day 12 post-reproductive adult with yolk distributed throughout the body. **c**, Graph depicting scores of the yolk redistribution phenotype as determined with a YP170/GFP reporter protein; y-axis, percentage of animals in a given category; x-axis, days (total number scored). Blue represents localization only to oocytes; yellow represents localization to oocytes and body cavity; green represents localization to body cavity only. **d**, Representative muscle nuclei of the wild type and the *age-1(hx546)* mutant expressing nuclearly targeted  $p_{myo-3}$ GFP. Although nuclei were chosen as average for their class, note that nuclear GFP changes with stochastic onset and a fair degree of variation in severity. Larger data montages used in blind tests and test results are provided in Supplementary Fig. 2. Note that in the *age-1(hx546)* background, there is a delay in the onset and progression of nuclear changes (days 7, 9 and 11), but differences are no longer clearly distinguishable after day 14.

geal muscle sectors can sporadically appear darkened and abnormal, a phenomenon that suggests a stochastic component to muscle degeneration (Fig. 3l, m).

Taken together, our results indicate that, like humans, ageing nematodes suffer from sarcopenia, the progressive loss of muscle mass and muscle function over time with mid-life onset.

### Stochastic origins of catastrophic events in other tissues

Electron-microscopic data indicate that many additional cell types (such as hypodermis and intestine), but not all (the kidney-like canal cell and some oocytes), exhibit age-related deterioration (see Supplementary Fig. 4). A decline in these cell types also seems to be stochastic, much as muscle decline does. Overall, our survey indicates that ageing affects different cell types at different rates in *C. elegans* and that stochastic events are factors in the age-related decline of multiple tissue types. It might be noteworthy that hypodermis and intestine often suffer random but extreme local crises, apparently associated with plasma membrane disruption, which might contribute to the death of the animal in advanced age (see Supplementary Information Discussion on causes of death in *C. elegans* and roles of cell death in ageing).

### Unregulated biosynthesis in post-reproductive *C. elegans*

Our GFP reporter/electron-microscopic analysis yielded several examples indicative of unregulated biosynthesis late in life. For example, we and others<sup>17</sup> have noted marked accumulation of lipid inclusions in intestine (Supplementary Figs 4c, d and 5b), muscle (Fig. 3j) and hypodermis (Supplementary Fig. 5c–e). We were also struck by a marked thickening of the *C. elegans* cuticle during ageing (Fig. 3n, o). Increases in cuticle thickness can reach 10-fold that in young adults in some locales, indicating that hypodermal cells continue collagen synthesis well into adulthood, even though ageing animals have passed larval developmental moulting periods. (The cuticle of old animals is quite wrinkled, which might reflect the weakening of hypodermis and/or muscle.) Electron-microscopic data also revealed the accumulation of body-wide electron-dense material similar to that previously identified as yolk protein<sup>18</sup>. We used immunoelectron microscopy to confirm that yolk protein YP170 was distributed in electron-dense lipid-like droplets and large dark accumulations throughout the body cavity in older animals (Supplementary Fig. 5f). In addition, we could discern age-related yolk redistribution with the reporter YP170/GFP. In young animals, YP170/GFP is found almost exclusively in the intestine (where it is synthesized) as well as in late-stage oocytes (which accumulate it) and embryos (Fig. 4a), but as animals enter the post-reproductive period, we found YP170/GFP throughout the body cavity of the animal (Fig. 4b). Thus, yolk protein production continues (at least initially) in the absence of oogenesis in post-reproductive nematodes. Overall, the extensive accumulation of macromolecules, such as yolk proteins, cuticle proteins and lipid, suggest that in post-reproductive animals, a life-stage that has been subject to little (if any) natural selection pressure over time, biosynthesis/protein turnover is not tightly regulated like it is in developmental and reproductive phases.

### Longevity mutations delay onset of some biomarkers of ageing

Having identified several potential biomarkers associated with ageing *C. elegans* tissues, we initiated efforts to address the basic question of how mutations causing increased longevity affect tissue-specific aspects of ageing: do long-lived mutants exhibit delay, or suppression, of all biomarkers associated with ageing, or might only specific aspects of body/tissue decline be affected? To gain first insight into this question, we compared life-long expression of the two most consistent and markedly altered GFP reporter proteins that we identified, yolk protein YP170/GFP and the muscle nuclear reporter expressed from  $p_{myo-3}$ GFP/NLS, in wild-type and *age-1(hx546)* mutant backgrounds. *age-1* encodes a phosphatidyl-

inositol-3-OH kinase (PI(3) kinase) that acts downstream in the DAF-2 insulin-like receptor signalling to influence lifespan<sup>19</sup>. *age-1(hx546)* animals live 60–100% longer than wild type<sup>20</sup>. We categorized YP170/GFP distribution in ageing animals into three groups: fluorescence exclusively in eggs, fluorescence in eggs and body cavity, and fluorescence solely in the body cavity. When we compared wild-type and *age-1* backgrounds, we could find no significant differences in either the time of onset or the apparent extent of body-wide yolk diffusion over time (Fig. 4c), indicating that *age-1(hx546)* animals experience extended lifespan despite the fact that yolk protein becomes widely distributed throughout the body at the start of the post-reproductive period, as occurs in ageing wild-type animals. Thus, not all phenotypes associated with ageing are altered by the increased longevity mutation *age-1(hx546)*.

By contrast, when we examined changes in GFP distribution in muscle nuclei in the *age-1(hx546)* mutant background, we found that there was a significant delay in the onset and extent of nuclear GFP changes in comparison with wild-type animals (Fig. 4d). We reared  $p_{myo-3}$ GFP/NLS and *age-1*;  $p_{myo-3}$ GFP/NLS strains under identical conditions and collected photographs of every nucleus (to avoid sampling bias) from multiple nematodes from days 6 to 19. Representative nuclei are featured in Fig. 4d, but in view of the stochastic component to onset and extent of nuclear GFP redistribution we found it essential to compare large collections of nuclear photographs (Supplementary Figs 2a, c and d). Our analysis of more than 20 photographs for each time point indicated that at day 5 (young adulthood) there are no detectable differences between wild-type and *age-1* animals. By day 7, we see the onset of GFP patching in the wild type, but this is not evident in *age-1* animals. At day 9, we can find patching in both populations of nuclei but patching is clearly more extensive in the wild-type background. Differences persist until day 14/16, after which we can no longer readily distinguish between wild-type and *age-1* animals for this age-associated phenotype.

We conclude that *age-1(hx546)*, which enhances locomotory activity in ageing populations<sup>21</sup>, delays the onset of age-related muscle nuclear changes and suggest that the *age-1* PI(3) kinase might exert its effects on healthspan and longevity in part by prolonging muscle integrity.

### A strong stochastic component for age-related decline

Our analysis of cellular changes in ageing *C. elegans* revealed several remarkable aspects of nematode senescence. Key findings are that stochastic factors make a significant contribution to senescent decline and that different cell types deteriorate at markedly different rates, with the nervous system being spared extensive cellular decline while muscle undergoes a profound and progressive deterioration with mid-life onset. We also report that the increased longevity mutation *age-1(hx546)* can delay the onset of some, but not all, cellular features of ageing.

One striking aspect of the biology of the ageing of *C. elegans* is the wide variability in both the time of onset and the rate of apparent deterioration within an isogenic population reared under uniform environmental conditions<sup>9,22</sup>. Although factors in the micro-environment or life histories of individuals (for example, the amount of time spent in food as opposed to near it) could profoundly affect ageing rates, we repeatedly observed a stochastic occurrence of cellular demise within the same cell types of individual animals. The marked variation in cellular decline is probably attributed to random damage or failures. In providing evidence for significant stochastic influences on both the overall senescent decline of the organism and the degeneration of individual cells within a single *C. elegans* (an organism in which there is virtually no genetic or developmental variation between animals), our data support a key premise of the ‘disposable soma’ theory of ageing, which postulates that damage caused by chance events is a major contributor to ageing soma<sup>23–25</sup>. Another premise of this theory is

that the genes that influence ageing and lifespan should primarily be involved in maintenance and repair of the soma<sup>23–25</sup>, and all characterized *C. elegans* increased-longevity mutations tested increase resistance to various stresses<sup>3,26</sup>. Given that stochastic contributions also affect ageing in other animals<sup>27,28</sup>, we emphasize that an understanding of stochastic components will be required for a full description of ageing in both *C. elegans* and higher organisms<sup>27,29</sup>.

### Maintenance of nervous-system integrity in animal ageing

After scoring thousands of individual *C. elegans* neurons during ageing, we conclude that neurons maintain their structural integrity for the duration of the lifespan. At the cellular level, we find no evidence of cell loss or axon degeneration, even in animals with severely compromised mobility. Previous analyses of ageing in other nematodes also failed to note significant neuronal deterioration with age<sup>17</sup>. Similarly, neuronal counts in fly eye<sup>30</sup> and antenna<sup>31</sup> provided no evidence for neuronal loss as a significant component of *Drosophila* ageing. Recent investigations using stereological imaging for quantification have generally concluded there is little neuronal loss associated with normal ageing in specific human brain regions studied, challenging long-held notions about significant loss of mammalian brain neurons with age (reviewed in ref. 32). The basic maintenance of the cellular integrity of nervous systems might be a common feature of metazoan ageing, although given documented differences in neuronal integrity among various ageing rodent inbred strains<sup>33</sup>, it is clear that genetic factors can influence neuronal health and function in aged animals.

Because extensive neuronal loss seems less of a significant factor in age-related cognitive and motor deficits in humans, experimental attention has turned to the evaluation of synaptic function in higher organisms. A higher-resolution examination of synaptic function in nematodes (including quantification of synaptic proteins in synapses, characterization of neuronal transcripts, and detailed ultrastructural analysis of synaptic integrity in specific behavioural classes over time) will be required to identify molecular and subcellular changes that accompany neuronal ageing in *C. elegans*. Similarly, detailed changes at the neuromuscular junction remain to be examined (see Supplementary Information Discussion).

### Like humans, *C. elegans* experience sarcopenia

*C. elegans* body wall muscle is considered to be analogous to human skeletal muscle in several respects<sup>34</sup>. In humans, loss of muscle mass is associated with a shrinkage in the sizes of the fused muscle cells, thought to be due to a decrease in the cytoplasmic volume of the cell<sup>35</sup>. Our electron-microscopic analysis provides clear evidence of cytoplasmic volume loss and a gross decrease in myofibril numbers in body wall muscle in aged animals. In rats, sarcomere integrity is progressively compromised with age such that the packing geometry of the sarcomere fibres is generally loosened, and fraying and loss of direction of individual muscle fibres occur<sup>36</sup>. Our analysis of both GFP-tagged myosin and electron micrographs in ageing nematodes provides clear evidence of the loosening of sarcomere geometry, the fraying of individual sarcomeres and the loss of direction of individual sarcomeres. *Drosophila* flight muscle also exhibits signs of age-related deterioration<sup>37</sup>; we therefore speculate that sarcopenia might emerge as another common feature in ageing metazoans.

### The *age-1*/PI(3) kinase influences sarcopenia

Disruption of the *age-1*/PI(3) kinase, a downstream signalling component in the DAF-2 insulin-like signalling pathway, delays the onset of GFP-reported nuclear deterioration in muscle and extends healthspan. Our work implicates *age-1*/PI(3) kinase as the first genetic factor influencing nematode sarcopenia and, by analogy, we suggest that PI(3) kinase is a candidate for a similar role in human sarcopenia. Interestingly, *age-1* (*hx546*) effects on the muscle

nuclei are first evident in mid-life, beginning near the post-reproductive transition. Our results reinforce the idea that mid-life events might have a significant impact on healthspan and longevity<sup>38</sup>. Also noteworthy is the recent finding that *daf-2* (which encodes an insulin-like receptor that influences lifespan<sup>2</sup>) might normally influence the rate of ageing in several tissues<sup>39</sup>. Perhaps several components of the insulin-like pathway influence sarcopenia.

### How does tissue ageing relate to longevity?

Signals derived from specific tissues that affect the lifespan phenotype have been reported for insulin-like signalling<sup>40</sup> as well as for the *C. elegans* somatic gonad and germ line<sup>38,41</sup>. It is not yet clear how these signals influence tissue-specific aspects of ageing, such as muscle decline, nor is it known whether, or how, muscle decline influences longevity. Expression of *age-1* in muscle alone in an otherwise *age-1* mutant background cannot rescue the lifespan extension phenotype, but it can correct lipid metabolism defects<sup>40</sup>. We shall need to determine whether *age-1* expressed solely in muscle rescues sarcopenia and to characterize how the various increased longevity mutants affect tissue-specific aspects of ageing to address the question of how the health of different tissues relates to the lifespan of the organism.

### Lack of gene regulation in post-reproductive life

Our analysis of the cell biology of *C. elegans* ageing revealed multiple lines of evidence indicating that gene expression and/or protein turnover is not coordinated with biological need during the post-reproductive period of life. At the ultrastructural level, we confirmed extensive lipid, lipofuscin and yolk accumulation and we noted that the collagenous *C. elegans* cuticle markedly thickens in aged animals. In terms of cell-specific GFP reporters, we noted that all of the 12 reporters we examined remained detectable over the lifespan. Our observations raise the possibility that many genes expressed at the end of the reproductive period might continue to be expressed long into the lifespan. Because selective pressure is thought to decline progressively with age<sup>29</sup> and should be effectively non-existent on post-reproductive *C. elegans*, one might predict that biosynthesis might be poorly regulated during post-reproductive life so that a 'left-on' profile of gene expression could endure<sup>42</sup>. Consistent with this, no major changes in *C. elegans* proteins resolved on two-dimensional gels occur over time<sup>43</sup>. We speculate that non-regulated biosynthesis might contribute to the senescent decline of *C. elegans* by causing the continued production of irrelevant macromolecules. We note that for most LacZ-tagged markers examined in *Drosophila*, genes continue to be expressed into old age<sup>31,44</sup> (*wg* is an exception<sup>44</sup>). Possibly, the 'expression left-on' phenotype might be a general feature of ageing organisms released from selective pressures.

Even when some aspects of the 'expression left-on' phenotype are operative, increased-longevity mutant *age-1* (*hx546*) exhibits delayed decline in both locomotory activity and nuclear muscle changes. Thus, manipulation of only a subset of age-related phenotypes might suffice to provide significant adjustments to quality of life. Analysis of processes that affect ageing in specific tissues could therefore provide useful clues for combating some deleterious aspects of human ageing. □

### Methods

#### Strains and media

All nematodes were maintained at 20 °C as described<sup>45</sup>. Strains used were: IM175 *unc-119*/GFP (W. Wadsworth, unpublished observations); ZB154 *zdl5* *p<sub>unc-4</sub>*-GFP (S. Clark, unpublished observations); NW1099 *evl5* *b2a* [*P<sub>unc-129</sub>*/GFP *pM1186*(*dpy-20*(+))]<sup>13</sup>; PD4251 *ccl54251* (*P<sub>myo-3</sub>*-GFP, *dpy-20* (+)); RW1596 *myo-3*(*st386*); *P<sub>myo-3</sub>*-GFP, *rol-6*(*su1006*)<sup>16</sup>; DH1033 *bls1* [*YP170*/GFP, *rol-6*(*su1006*)]; *sqt-1*(*sc103*); IAO19 (*P<sub>col-12</sub>*/GFP, *rol-6*(*su1006*)); EG1653 *oxls22* (*P<sub>unc-49</sub>*/GFP; *lin-15*(+)); *rhl52* *pat-3*/GFP; TJ1052 *age-1* (*hx546*) II; BE13 *sqt-1*(*sc13*) II; and N2. Double-mutant strains were constructed by standard genetic approaches; *sqt-1* was used as a linked marker to track *age-1* (*hx546*) in crosses; longevity phenotype was confirmed.

**Age synchronization and behavioural scoring of ageing nematodes**

To age-synchronize nematodes, 5–10 gravid adults were plated on two to four plates to lay eggs for 2–4 h and then removed; the day of egg deposition was scored as day 0. When animals matured to the L4 larval stage, they were distributed (10 nematodes per plate) and scored every 1–3 d for classes A, B and C as described in the text. Animals that did not respond to prodding with a wire and showed no pharyngeal pumping were scored as dead.

**Microscopy techniques**

After scoring for behavioural class, animals were fixed and embedded by standard methods<sup>46</sup>. Thin sections were collected in transverse or longitudinal aspects and examined on a Philips CM10 transmission electron microscope. Results were drawn from over 500 electron micrographs, drawn primarily from a total of two class A, six class B and three class C animals. Young adult wild-type animals were available from 25 animals in our archival collection. Immunocytochemistry was performed by a post-embedding procedure as described by Paupard *et al.*<sup>47</sup>. Gold-linked secondary antibodies were imaged by electron microscopy on the thin sections of aldehyde-fixed aged animals, using primary antibodies against yolk protein<sup>47</sup>.

For GFP analysis, age-synchronized nematodes were transferred to new plates at 2-day intervals. For each strain, the animals were reared under identical temperature and growth conditions for comparison. For several lines we found that the GFP strains used for these experiments had slightly shorter lifespans than the N2 strain, but we always continued to the end of the lifespan. At several intervals (usually every 2 or 3 days), 5–10 animals were analysed by fluorescence microscopy. Animals were observed and photographed with a higher-magnification fluorescent microscope (Zeiss) with a Real-14 Precision Digital camera attachment. Observations of GFP expression were recorded and colour images were taken for the documentation of results with Magnafire software.

**Dye-filling experiments**

Stock dye solution (50 µl; 20 mg ml<sup>-1</sup> of 5-fluorescein isothiocyanate (FITC) in dimethylformamide) was mixed with 200 µl of M9 buffer and applied to a seeded nematode growth medium plate for 2–12 h before testing<sup>48</sup>. Age-synchronized nematodes were placed on FITC-containing plates for 4–12 h and then transferred to seeded plates without dye for at least 1 h to remove excess FITC from the intestine and from the outside of the animal. Nematodes were mounted and observed as described above for GFP observation, but with a FITC filter.

Received 22 April; accepted 4 September 2002; doi:10.1038/nature01135.

1. Vanfleteren, J. R. & Braeckman, B. P. Mechanisms of life span determination in *Caenorhabditis elegans*. *Neurobiol. Aging* **20**, 487–502 (1999).
2. Braeckman, B. P., Houthoofd, K. & Vanfleteren, J. R. Insulin-like signaling, metabolism, stress resistance and aging in *Caenorhabditis elegans*. *Mech. Ageing Dev.* **122**, 673–693 (2001).
3. Lithgow, G. J. & Walker, G. A. Stress resistance as a determinate of *C. elegans* lifespan. *Mech. Ageing Dev.* **123**, 765–771 (2002).
4. Sulston, J. E. & Horvitz, H. R. Post embryonic cell lineages of the nematode *Caenorhabditis elegans*. *Dev. Biol.* **56**, 110–156 (1977).
5. White, J. G., Southgate, E., Thomson, J. N. & Brenner, S. The structure of the nervous system of *Caenorhabditis elegans*. *Phil. Trans. R. Soc. Lond. B* **314**, 1–340 (1986).
6. Klass, M. R. Aging in the nematode *Caenorhabditis elegans*: major biological and environmental factors influencing life span. *Mech. Ageing Dev.* **6**, 413–429 (1977).
7. Bolanowski, M. A., Jacobson, L. A. & Russell, R. L. Quantitative measures of aging in the nematode *Caenorhabditis elegans*. II. Lysosomal hydrolases as markers of senescence. *Mech. Ageing Dev.* **21**, 295–319 (1983).
8. Driscoll, M. Cell death in *C. elegans*: Molecular insights into mechanisms conserved between nematodes and mammals. *Brain Pathol.* **6**, 411–425 (1996).
9. Johnson, T. E. Aging can be genetically dissected into component processes using long-lived lines of *Caenorhabditis elegans*. *Proc. Natl Acad. Sci. USA* **84**, 3777–3781 (1987).
10. Hall, D. H. *et al.* Neuropathology of degenerative cell death in *C. elegans*. *J. Neurosci.* **17**, 1033–1045 (1997).
11. Maduro, M. & Pilgrim, D. Identification and cloning of unc-119, a gene expressed in the *Caenorhabditis elegans* nervous system. *Genetics* **141**, 977–988 (1995).
12. Mitani, S., Du, H., Hall, D. H., Driscoll, M. & Chalfie, M. Combinatorial control of touch receptor neuron expression in *Caenorhabditis elegans*. *Development* **119**, 773–783 (1993).
13. Colavita, A., Krishna, S., Zheng, H., Padgett, R. W. & Culotti, J. G. Pioneer axon guidance by UNC-129, a *C. elegans* TGF-β. *Science* **281**, 706–709 (1998).
14. Apfeld, J. & Kenyon, C. Regulation of lifespan by sensory perception in *Caenorhabditis elegans*. *Nature* **402**, 804–809 (1999).
15. Perkins, L. A., Hedgecock, E. M., Thomson, J. N. & Culotti, J. G. Mutant sensory cilia in the nematode *Caenorhabditis elegans*. *Dev. Biol.* **117**, 456–487 (1986).
16. Campagnola, P. J. *et al.* Three-dimensional high-resolution second-harmonic generation imaging of endogenous structural proteins in biological tissues. *Biophys. J.* **82**, 493–508 (2002).
17. Epstein, J., Himmelhoch, S. & Gershon, D. Studies on ageing in nematodes. III. Electron microscopical studies on age-associated cellular damage. *Mech. Ageing Dev.* **1**, 245–255 (1972).
18. Hall, D. H. *et al.* Ultrastructural features of the adult hermaphrodite gonad of *Caenorhabditis elegans*: relations between the germ line and soma. *Dev. Biol.* **212**, 101–123 (1999).
19. Kimura, K. D., Tissenbaum, H. A., Liu, Y. & Ruvkun, G. *daf-2*, an insulin receptor-like gene that regulates longevity and diapause in *Caenorhabditis elegans*. *Science* **277**, 942–946 (1997).
20. Friedman, D. B. & Johnson, T. E. A mutation in the *age-1* gene in *Caenorhabditis elegans* lengthens life and reduces hermaphrodite fertility. *Genetics* **118**, 75–86 (1988).

21. Duhon, S. A. & Johnson, T. E. Movement as an index of vitality: comparing wild type and the *age-1* mutant of *Caenorhabditis elegans*. *J. Gerontol. A Biol. Sci. Med. Sci.* **50**, B254–B261 (1995).
22. Bolanowski, M. A., Russell, R. L. & Jacobson, L. A. Quantitative measures of aging in the nematode *Caenorhabditis elegans*. I. Population and longitudinal studies of two behavioral parameters. *Mech. Ageing Dev.* **15**, 279–295 (1981).
23. Kirkwood, T. B. Evolution of ageing. *Nature* **270**, 301–304 (1977).
24. Kirkwood, T. B. Human senescence. *BioEssays* **18**, 1009–1016 (1996).
25. Kirkwood, T. B. Changing complexity in aging: a metric not an hypothesis. *Neurobiol. Aging* **23**, 21–22 (2002).
26. Johnson, T. E. *et al.* Relationship between increased longevity and stress resistance as assessed through gerontogene mutations in *Caenorhabditis elegans*. *Exp. Gerontol.* **36**, 1609–1617 (2001).
27. Finch, C. E. & Kirkwood, T. B. L. *Chance, Development, and Aging* (Oxford Univ. Press, New York, 2000).
28. Sozou, P. D. & Kirkwood, T. B. A stochastic model of cell replicative senescence based on telomere shortening, oxidative stress, and somatic mutations in nuclear and mitochondrial DNA. *J. Theor. Biol.* **213**, 573–586 (2001).
29. Kirkwood, T. B. Evolution of ageing. *Mech. Ageing Dev.* **123**, 737–745 (2002).
30. Leonard, D. S., Bowman, V. D., Ready, D. F. & Pak, W. L. Degeneration of photoreceptors in rhodopsin mutants of *Drosophila*. *J. Neurobiol.* **23**, 605–626 (1992).
31. Helfand, S. L. & Naprta, B. The expression of a reporter protein, β-galactosidase, is preserved during maturation and aging in some cells of the adult *Drosophila melanogaster*. *Mech. Dev.* **55**, 45–51 (1996).
32. Morrison, J. H. & Hof, P. R. Life and death of neurons in the aging brain. *Science* **278**, 412–419 (1997).
33. Jucker, M., Bondolfi, L., Calhoun, M. E., Long, J. M. & Ingram, D. K. Structural brain aging in inbred mice: potential for genetic linkage. *Exp. Gerontol.* **35**, 1383–1388 (2000).
34. Waterston, R. H. *The Nematode: Caenorhabditis elegans* (ed. Wood, W. B.) 281–337 (Cold Spring Harbor Laboratory Press, Cold Spring Harbor, NY, 1988).
35. Hughes, S. M. & Schiaffino, S. Control of muscle fibre size: a crucial factor in ageing. *Acta Physiol. Scand.* **167**, 307–312 (1999).
36. Fujisawa, K. Some observations on the skeletal musculature of aged rats. Part 2. Fine morphology of diseased muscle fibres. *J. Neurol. Sci.* **24**, 447–469 (1975).
37. Takahashi, A., Philpott, D. E. & Miquel, J. Electron microscope studies on aging *Drosophila melanogaster*. 3. Flight muscle. *J. Gerontol.* **25**, 222–228 (1970).
38. Arantes-Oliveira, N., Apfeld, J., Dillin, A. & Kenyon, C. Regulation of life-span by germ-line stem cells in *Caenorhabditis elegans*. *Science* **295**, 502–505 (2002).
39. Garigan, D. *et al.* Genetic analysis of tissue aging in *Caenorhabditis elegans*. A role for heat-shock factor and bacterial proliferation. *Genetics* **161**, 1101–1112 (2002).
40. Wolkow, C. A., Kimura, K. D., Lee, M. S. & Ruvkun, G. Regulation of *C. elegans* life-span by insulin like signaling in the nervous system. *Science* **290**, 147–150 (2000).
41. Hsin, H. & Kenyon, C. Signals from the reproductive system regulate the lifespan of *C. elegans*. *Nature* **399**, 362–366 (1999).
42. Lund, J. *et al.* Global profiles of aging in *Caenorhabditis elegans*. *Curr. Biol.* **12**, 1566–1573 (2002).
43. Johnson, T. E. & McCaffrey, G. Programmed aging or error catastrophe? An examination by two-dimensional polyacrylamide gel electrophoresis. *Mech. Ageing Dev.* **30**, 285–297 (1985).
44. Rogina, B., Vaupel, J. W., Partridge, L. & Helfand, S. L. Regulation of gene expression is preserved in aging *Drosophila melanogaster*. *Curr. Biol.* **8**, 475–478 (1998).
45. Lewis, J. A. & Fleming, J. T. *Caenorhabditis elegans: Modern Biological Analysis of an Organism* (eds Epstein, H. F. & Shakes, D. C.) 4–27 (Academic, San Diego, 1995).
46. Hall, D. H. Electron microscopy and three-dimensional image reconstruction. *Methods Cell Biol.* **48**, 395–436 (1995).
47. Paupard, M. C., Miller, A., Grant, B., Hirsh, D. & Hall, D. H. Immuno-EM localization of GFP-tagged yolk proteins in *C. elegans* using microwave fixation. *J. Histochem. Cytochem.* **49**, 949–956 (2001).
48. Hedgecock, E. M., Culotti, J. G., Thomson, J. N. & Perkins, L. A. Axonal guidance mutants of *Caenorhabditis elegans* identified by filling sensory neurons with fluorescein dyes. *Dev. Biol.* **111**, 158–170 (1985).

**Supplementary Information** accompanies the paper on Nature’s website (<http://www.nature.com/nature>).

**Acknowledgements** We thank the following people for providing the following strains used in this study: B. Wadsworth for IM175, S. Clark for ZB154, R. Padgett for NW1099, A. Fire for PD4251, P. Hoppe and B. Waterston for RW1596, B. Grant for DH1033, I. Johnstone for IA019, E. Jorgensen for EG1653, and J. Plenefisch for *rhs2*. We also thank the *Caenorhabditis* Genetics Center funded by NIH NCCR for the TJ1052 and BE13 strains. We thank G. Stepney, T. Stepney and K. Nguyen for help with electron microscopy; B. Levine and A. Melendez for helpful discussions about autophagy in *C. elegans*; G. Patterson and B. Grant for critical reading of this manuscript; and T. Johnson and D. Wu for advice about the analysis of behavioural class as a predictor of life expectancy. This work was supported by grants from the National Institute of Neurological Disorders and Stroke and the National Institute on Aging to M.D., and the Center for *C. elegans* Anatomy was supported by a grant from the NIH Division of Research Resources to D.H.

**Competing interests statement** The authors declare that they have no competing financial interests.

**Correspondence** and requests for materials should be addressed to M.D. (e-mail: driscoll@mcbcl.rutgers.edu) or D.H.H. (e-mail: hall@accomm.yu.edu).